THE JOURNAL OF PHYSICAL CHEMISTRY A

Article

pubs.acs.org/JPCA

Secondary Organic Aerosol Formation via the Isolation of Individual Reactive Intermediates: Role of Alkoxy Radical Structure

Anthony J. Carrasquillo,[†] James F. Hunter,[†] Kelly E. Daumit,[†] and Jesse H. Kroll*[,†,‡]

[†]Department of Civil and Environmental Engineering and [‡]Department of Chemical Engineering, Massachusetts Institute of Technology, Cambridge, Massachusetts 02139, United States

Supporting Information

ABSTRACT: The study of the chemistry underlying secondary organic aerosol (SOA) formation is complicated by the large number of reaction pathways and oxidation generations available to a given precursor species. Here we simplify such complexity to that of a single alkoxy radical (RO), by forming SOA via the direct photolysis of alkyl nitrite (RONO) isomers. Chamber experiments were conducted with 11 C_{10} RONO isomers to determine how the position of the radical center and branching of the carbon skeleton influences SOA formation. SOA yields served as a probe of RO reactivity, with lower yields indicating that fragmentation reactions dominate and higher yields suggesting the predominance of RO isomerization. The largest yields were from straight-chain isomers, particularly those with radical centers located toward the terminus of the molecule. Trends in SOA yields can be explained in terms of two major effects: (1) the relative importance of isomerization and fragmentation reactions, which control the distribution of products, and (2) differences in volatility among the various isomeric products formed. Yields from branched isomers, which were low but variable, provide insight into the degree of fragmentation of the alkoxy radicals; in the case of the two β-substituted alkoxy radicals, fragmentation appears to occur to a greater extent than predicted by structure−activity relationships. Our results highlight how subtle differences in alkoxy radical structure can have major impacts on product yields and SOA formation.

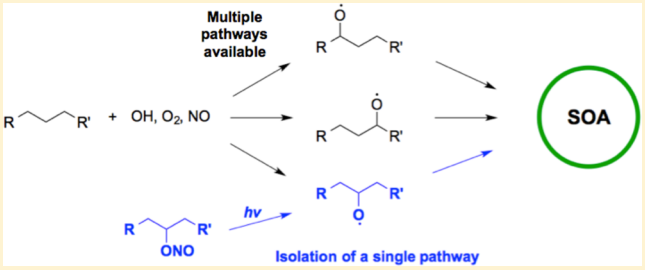

INTRODUCTION

Organic aerosol (OA) particles have important implications for human health, visibility, and climate; however, our ability to accurately predict ambient OA loadings, chemical composition, and properties is limited.[1−3] Particularly uncertain is the chemistry associated with secondary organic aerosol (SOA), formed from the oxidation of gas-phase VOCs and the subsequent condensation of low-volatility products. SOA formation is immensely complex, involving a large number of chemical species, reaction pathways, and oxidation generations.[3,4] This chemical complexity poses major challenges in understanding the detailed chemistry and specific reaction pathways that govern SOA formation and evolution, particularly when the reaction of a single oxidant with a single VOC can lead to the formation of a multitude of products.

Figure 1 illustrates the large number of reaction pathways and intermediates possible for even a very simple reaction system, the oxidation of an *n*-alkane by the OH radical. The reaction is initiated by H-abstraction by OH at one of several sites, followed by O_2 addition to form a number of distinct alkylperoxy radicals (RO_2, not shown). In the presence of NO these will form organonitrate ($RONO_2$, not shown) species or alkoxy (RO) radicals. The RO radicals are important branch points in oxidation reactions, and for large species will either fragment or isomerize. If the resulting products are sufficiently low in volatility, they will partition into the aerosol phase; otherwise, they will continue to react in the gas phase and form later-generation oxidation products that may themselves condense.[5] The resulting aerosol thus contains many product species, formed by numerous pathways over several generations of oxidation.

To simplify this complex chemistry, we recently demonstrated the utility of forming SOA by the direct photolytic generation of a single organic radical species.[6] This approach limits both the number of reactive pathways available (because only one radical species is formed) and the number of oxidation generations (because no oxidant is added). In that initial work, alkyl iodides (RI) were photolyzed at 254 nm in the presence of oxygen to give an alkylperoxy radical (RO_2). Here we expand this approach to a second key intermediate, the alkoxy radical, by the photolysis of alkyl nitrites (RONO):

$$\mathrm{RONO} + h\nu \rightarrow \mathrm{RO} + \mathrm{NO} \qquad (1)$$

Reaction 1 generally occurs in the 300−400 nm range and therefore involves much lower-energy photons than required for RI photolysis.[7,8] RO radicals may still be initially formed vibrationally[9] or electronically[7] excited, but for the large (C_{10}) species considered here, collisional deactivation by bath gas

Received: July 1, 2014
Revised: August 21, 2014
Published: August 22, 2014

   dx.doi.org/10.1021/jp506562r | J. Phys. Chem. A 2014, 118, 8807−8816

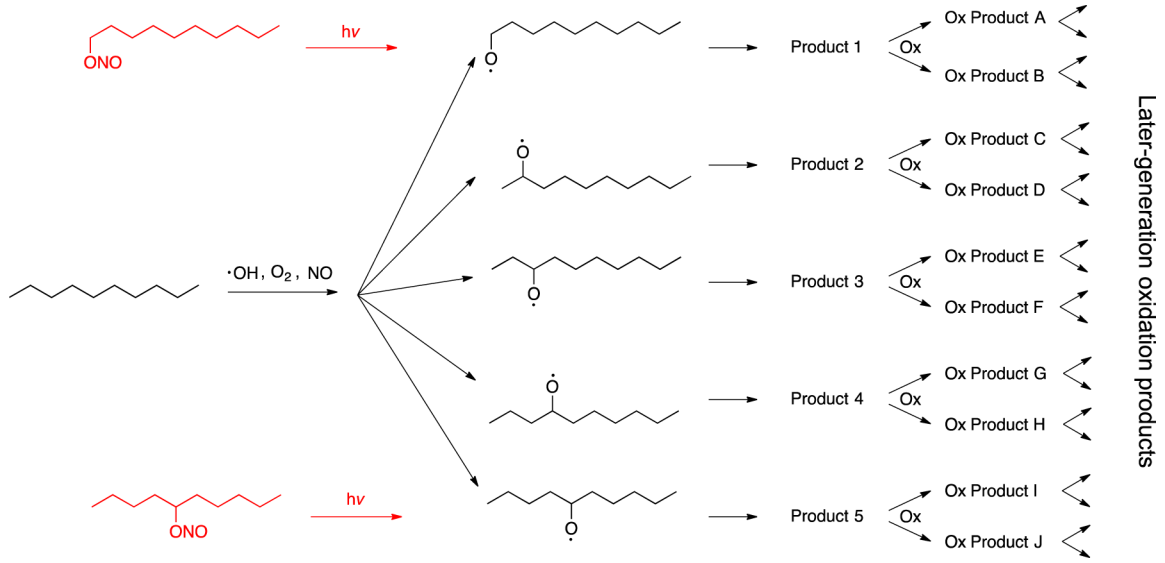

Figure 1. Formation of alkoxy radical isomers from *n*-decane. The OH radical can abstract any available H, yielding a distribution of five different radical isomers that then react to form a wide range of fragmentation or isomerization products; these then can oxidize further to form new products. Alkyl nitrite photolysis, shown in red, yields one specific alkoxy radical, with little secondary oxidation, greatly limiting the number of products formed.

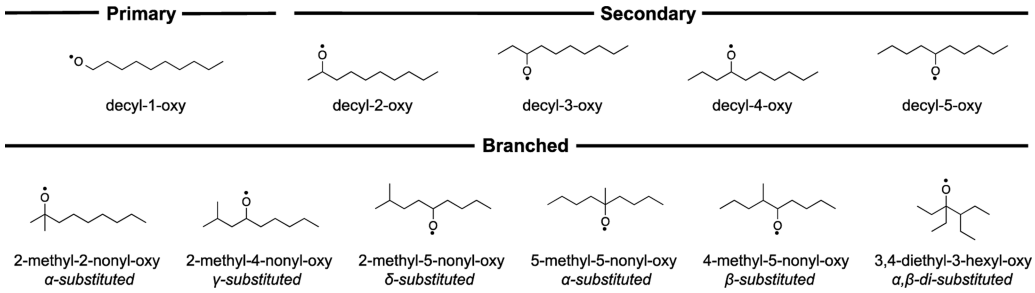

Figure 2. Alkoxy radical isomers examined in this study, listed according to their structural characterization (primary, secondary, or branched).

molecules is likely to remove this excess energy prior to reaction.[8] In addition, because the NO photofragment is far less reactive than I atoms formed from RI photolysis, any undesired (and uncertain) secondary chemistry is less likely than in our previous work.

In studies of OH + alkanes under high-NO conditions, Ziemann and co-workers have shown that the chemistry of alkoxy radicals is crucial in determining the yields and composition of SOA.[5,10,11] Such chemical systems can involve a complex mixture of several RO isomers. Here, using the photolysis of a series of C_{10} RONO isomers, we are able to examine RO radical chemistry in even more detail, by isolating the role of individual alkoxy radical species in SOA formation. Furthermore, in the absence of an added oxidant, the effects of multigenerational oxidative chemistry are minimized. The study of aerosol formation from individual alkoxy radical isomers thus allows for a highly detailed examination of the role of chemical structure (position and degree of substitution of the radical center) on SOA yields and composition.

EXPERIMENTAL SECTION

Selection and Synthesis of Alkyl Nitrite Species. RONO species are not commercially available, and so were synthesized in the laboratory. This synthesis, described below, requires the corresponding alcohol as the starting material; a series of C_{10} RONO isomers (formula $C_{10}H_{21}ONO$) was chosen on the basis of the large number of precursor alcohols available. The C_{10} alcohols used are 1-decanol and 2-decanol (Sigma-Aldrich), 3-decanol, 4-decanol, 5-decanol, 2-methyl-5-nonanol, 2-methyl-4-nonanol, 4-methyl-5-nonanol, 2-methyl-2-nonanol, 5-methyl-5-nonanol, and 3,4-diethyl-5-hexanol (Chemsampco). The alkoxy radicals formed from the 11 C_{10} nitrite isomers synthesized are listed in Figure 2. These radicals are grouped by degree of substitution: primary (straight-chain molecules with the radical center at the terminal carbon atom), secondary (straight-chain molecules with the radical center at one of the secondary/internal carbon atoms), and branched (molecules with at least one methyl or ethyl group branching off the carbon chain).

Synthesis of the nitrites was carried out via O-nitrosation of the alcohol.[12] In this procedure, all glassware, laboratory utensils, and aluminum foil were combusted at 550 °C for 10 h to remove all organic contaminants. Sodium nitrite (Sigma-Aldrich) and the alcohol were combined in a 1.1:1.0 molar ratio and stirred with a magnetic stirrer at 10 °C. To this mixture was added chilled 6 M sulfuric acid (Sigma-Aldrich) dropwise until a 0.5:1.0 acid:-alcohol molar ratio was achieved. The resulting clear yellow liquid was dried over sodium sulfate (Sigma-Aldrich) and neutralized with excess sodium bicarbonate (Sigma-Aldrich). Purity was confirmed by analysis with GC-FID and UV−vis. For GC analysis, 1 μL of nitrite solution (1 μg RONO/1 mL hexane) was injected into an Agilent 7890 GC-FID (50 m, 0.25 mm i.d. DB-5 column; held at 40 °C for 3 min, then ramped to 250 °C at 20 °C/min), which provided sufficient separation of the RONO (10−12 min retention time) from the precursor alcohol (12−14

dx.doi.org/10.1021/jp506562r | J. Phys. Chem. A 2014, 118, 8807−8816

min retention time). For all syntheses, the ratio of FID signals for the RONO compound to the unreacted alcohol was >95:1, indicating a conversion of at least 95% of the starting material to the nitrite. Confirmation of conversion to RONO was also made by UV−vis spectroscopy of the same RONO mixture, with measured spectra similar to those reported by Heicklen.[8] Synthesized RONO species were stored in the dark and used within 1−2 h of synthesis to maintain its integrity.

Chamber Studies. Experiments were conducted in a 1 m^3 Teflon PFA (40 mil) chamber (Ingeniven) surrounded by four 40 W black lights (Sylvania BL350). The spectral output of these lamps (300−400 nm, centered at ∼350 nm) overlaps well with the absorption spectrum of RONO species,[8] allowing for efficient photolysis. The chamber was operated at a constant volume such that the air sampled was balanced with dry (RH < 7%) makeup air from a clean air generator (Aadco, <5 ppb_v hydrocarbons). Gas-phase RONO concentration was monitored with a GC-FID (SRI 8610C) equipped with a Tenax trap and a 30 m 0.53 mm DB-5 column. Prior to each experiment, the chamber was flushed with clean air for a minimum of 10 h, giving a background particle concentration of <10 particles/cm^3.

The RONO species and a dilution tracer hexafluorobenzene (C_6F_6, Sigma-Aldrich) were injected into the chamber via a stream of air to attain initial chamber concentrations of 200 ppb_v and 40 ppb_v, respectively. For the experiments described here, high levels of NO (∼1 ppm) were added to the chamber, both to ensure that RO_2 + NO reactions dominate the RO_2 chemistry across all experiments and to inhibit the formation of O_3 and NO_3. Ammonium sulfate ($(NH_4)_2SO_4$) seed particles were added to promote condensation of low-volatility species onto particles, and also to correct for losses of particles to dilution or wall loss (as described below). Polydisperse $(NH_4)_2SO_4$ seed was generated by atomizing a 1 g/L aqueous solution with a constant output atomizer (TSI Instruments), dried by a drierite denuder, and neutralized using two ^{210}Po static eliminators (Nuclecel, 10 mCi) in series. To minimize the contribution of organic background from the seed, the aqueous $(NH_4)_2SO_4$ solution was extracted five times with high-purity dichloromethane (Omnisolv, VWR) and boiled for 4 h to remove any residual solvent. Seed surface area concentrations were high enough (1000−1800 $\mu m^2/cm^3$ at ∼30 $\mu g/m^3$) to inhibit new particle formation within the chamber. RONO, C_6F_6, NO, and seed particles were allowed to mix in the dark chamber for 30 min before the blacklights were turned on, initiating photochemistry. Data collection continued until particle growth finished.

Aerosol Composition. Particle composition was measured in real time using an Aerodyne high-resolution aerosol time-of-flight mass spectrometer (AMS),[13] run in "V mode" (resolving power of ∼3000) to maximize sensitivity. Time series for the major aerosol families (sulfate, organic, nitrate) were generated from high-resolution fitting of individual mass spectra, and elemental ratios of the organics (O/C, H/C, N/C) were determined using the approach described in Aiken et al.[14,15] Filter blanks were taken for 10 min at the start and end of every experiment to measure and correct for the gas-phase CO_2^+ signal within the AMS. All N from NO^+ and NO_2^+ were included in the calculation of N/C, because any nitrate formed is likely to be from organonitrates; however, only O atoms directly bonded to the carbon were included in the determination of O/C.

Yield Calculations. The time-dependent SOA yield (Y) is given by eq 2:

$$Y\ (\%) = \frac{\Delta c_{OA}(t)}{\Delta \mathrm{RONO}(t)\cdot 0.840}\cdot 100\% \qquad (2)$$

where $\Delta c_{OA}(t)$ is the increase in organic aerosol concentration ($\mu g/m^3$) and $\Delta \mathrm{RONO}(t)$ is the mass concentration of nitrite photolyzed (the multiplicative factor 0.840 is to exclude the mass of the NO photofragment from the yield calculation). $\Delta \mathrm{RONO}(t)$ is calculated as the difference between the initial amount present, $\mathrm{RONO}(t_0)$, and the amount remaining at time t, corrected for flushing using measured C_6F_6 concentrations. For all RONO measurements the FID calibration factor was determined by averaging the GC-FID response across all experiments at t_0 and equating this to 200 ppb_v.

The AMS and an SMPS (TSI model 3080) were used to determine organic aerosol formation (Δc_{OA}). Aerosol growth was corrected for wall loss and dilution using the method of Hildebrandt et al.,[16] in which the organic-to-sulfate mass ratio (as measured by the AMS) is scaled by the initial sulfate mass (calculated from the SMPS volume and a density of 1.77 g/cm^3). Because the sulfate mass concentration will change only by physical loss processes (deposition to the walls and flushing), this approach corrects for losses of organic particle mass to walls and dilution, losses of organic vapors to OA deposited on the chamber walls, and any changes to the AMS collection efficiency or sensitivity over the course of the experiment. This approach does not account for any partitioning of semivolatile species to the chamber walls,[17] an effect that might lower the measured yields; however, the overall trends are unlikely to be affected by such wall-loss processes.

RESULTS

Aerosol Formation and Yields. Results for a representative experiment, the photolysis of 200 ppb_v of decyl-3-nitrite, are shown in Figure 3. When the lights are turned on, RONO decays exponentially, with a decay constant of 2.1×10^{-4} s^{-1}. Photolysis rates for all nitrites are similar, with an average decay constant of 2.5×10^{-4} s^{-1} for all species studied. Significant GC interferences

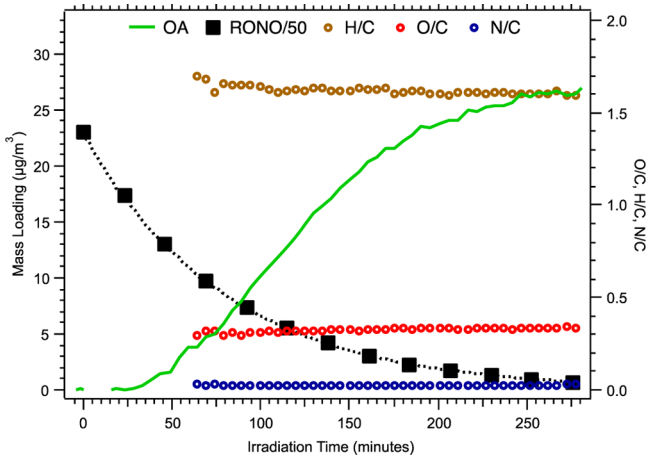

Figure 3. Time-dependent results from a representative alkoxy radical experiment, using decyl-3-nitrite as the precursor RONO species. GC-FID measurements of RONO concentrations (scaled by 1/50) are shown as black squares, with the exponential fit to the data as a dashed line. The organic aerosol mass concentration (c_{OA}), corrected for wall loss and dilution, is shown in green. Elemental ratios (O/C, H/C, and N/C) exhibit low signal-to-noise at low mass loadings and so are shown only after ∼4 $\mu g/m^3$ of OA is formed.

dx.doi.org/10.1021/jp506562r | J. Phys. Chem. A 2014, 118, 8807−8816

from gas-phase products with retention times similar to that of RONO preclude the direct measurement of RONO concentration after 3−5 h, so fitted values (dotted line in Figure 3) were used for all values of ΔRONO. Roughly 25 min after irradiation is initiated, OA mass concentration (c_{OA}) begins increasing. A significant amount of SOA is formed, with corrected loadings reaching a plateau of ∼25 $\mu g/m^3$ after 4−5 h. Also shown in Figure 3 are the elemental ratios of the SOA formed; these vary little over the course of the experiment and are discussed in detail in a later section.

SOA formation was observed for all alkoxy radical species studied, with the exception of the 3,4-diethyl-3-hexyloxy radical. Yield curves (plots of aerosol yield as a function of c_{OA}) for all alkoxy radicals that formed SOA are shown in Figure 4. Yields

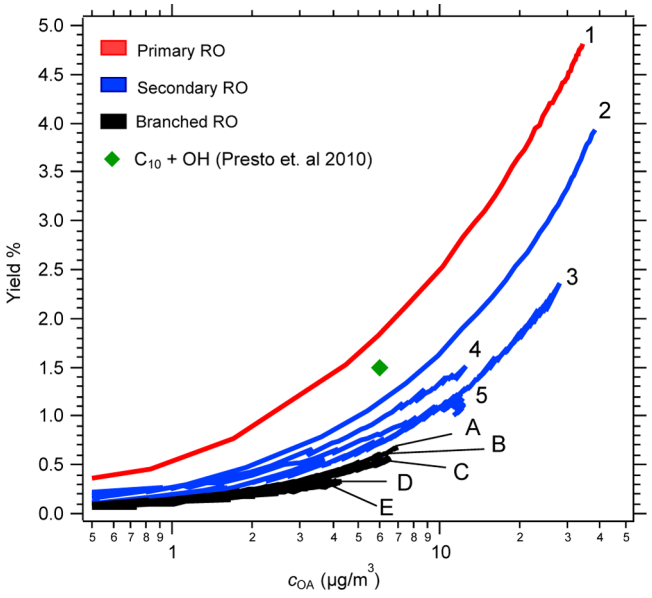

Figure 4. Yield % curves as a function of c_{OA} ($\mu g/m^3$) for the C_{10} alkoxy radical species studied. Curves are colored by structural type: red indicates the primary radical (1: decyl-1-oxy); blue the secondary radicals (2: decyl-2-oxy, 3: decyl-3-oxy, 4: decyl-4-oxy, and 5: decyl-5-oxy); and black the branched radicals (A: 2-methyl-2-nonyl-oxy, B: 2-methyl-4-nonyl-oxy, C: 2-methyl-5-nonyl-oxy, D: 5-methyl-5-nonyl-oxy, and E: 4-methyl-5-nonyl-oxy). No aerosol formation was observed from the 3,4-diethyl-3-hexyl-oxy radical. The SOA yield of the analogous reaction, *n*-decane + OH, as measured by Presto et al.[18] is shown as the green diamond. Yields from additional studies[19−21] are not shown here as they were conducted at higher c_{OA} levels.

(Y) from the three groups of alkoxy radicals decreased from $Y_{primary} > Y_{secondary} > Y_{branched}$. SOA yields for the straight-chain species generally decreased as the radical center was located closer to the center of the carbon skeleton ($Y_{decyl\text{-}1\text{-}oxy} > Y_{decyl\text{-}2\text{-}oxy} > Y_{decyl\text{-}4\text{-}oxy} > Y_{decyl\text{-}3\text{-}oxy} > Y_{decyl\text{-}5\text{-}oxy}$). The branched alkoxy radicals exhibited lower yields than the straight-chain isomers, with yields showing no obvious trend with the location of the branching methyl group relative to the radical center ($\alpha, \beta, \gamma, \delta$). No aerosol formation was observed from the α,β-disubstituted isomer (3,4-diethyl-3-hexyloxy). These results are examined in detail in the Discussion.

Product volatility distributions were derived from yield curves using the volatility basis set approach,[22] with fixed saturation vapor concentration (c^*) bins of 1, 10, and 100 $\mu g/m^3$. These bins span the range of c_{OA} accessed in this study, and thus including additional bins did not improve the fits significantly. The mass-based yields for each bin (α_1, α_{10}, and α_{100}) are listed in Table 1, both for the individual alkoxy radicals and for averages of all secondary and branched radicals.

Aerosol Composition. Elemental ratios (O/C, H/C, and N/C) of the SOA generated from all alkoxy radical species (averaged over the last 2 h of each experiment) are also given in Table 1. Because our determination of N/C is dominated by the NO^+ and NO_2^+ ions, here N/C is a measure of organonitrate abundance. Similarly, because reported O/C ratios do not include the two terminal O atoms bonded to the nitrate-N,[23] they account only for oxygen atoms directly bonded to the carbon skeleton, and thus represent a measure of the degree of carbon oxidation.

As illustrated in Figure 3, elemental ratios do not vary dramatically over the course of an experiment; on average, O/C and N/C values increased slightly (by <10% and ∼5% respectively) while H/C decreased (by ∼3−5%) over 2−3 h of irradiation. This absence of "aging" is expected for the present system, whose chemistry is dominated by a single rate-limiting reaction step (the photolysis of the RONO species); the subsequent drift toward slightly more oxidized products may result from secondary oxidation reactions (described below) or slow repartitioning effects that result from dilution of the chamber.

SOA formed from the primary alkoxy radical is less oxidized (O/C = 0.19, H/C = 1.62) than SOA formed from secondary and branched alkoxy radicals (average values: O/C = 0.25, H/C = 1.63). This corresponds to differences in the degree of functionalization of the carbon skeleton: assuming that condensed species retain their C_{10} carbon skeleton (i.e., that the SOA includes no fragmentation products), SOA from the primary alkoxy radical contains on average two oxygen-containing moieties per molecule, whereas the SOA from secondary and branched alkoxy radicals can have up to three such moieties per molecule on average. At the same time, the SOA formed from isomers with their radical centers closest to the terminus of the molecules tended to have the highest abundances of organonitrates (N/C of 0.05 for decyl-1-oxy and decyl-2-oxy vs ∼0.03 for all others). Because SOA from these isomers also had the lowest O/C values, nitrates appear to account for a relatively large fraction of the functional groups in the less-oxidized SOA.

DISCUSSION

Reaction Mechanism. Reaction pathways available to the alkoxy radicals studied in these experiments are shown in Figure 5. The top panel in Figure 5 shows the initial gas-phase reactions possible: the two key channels are isomerization (green arrows), which forms a hydroxyalkyl radical, and fragmentation (red arrows), which forms a carbonyl and an alkyl radical. A third channel, the reaction with O_2 to form a carbonyl and HO_2, is expected to be negligible for straight-chain species but can be significant for some of the branched isomers.[24] The isomerization pathway tends to form multifunctional, lower-volatility products (generally promoting SOA formation), whereas fragmentation forms two smaller, relatively volatile species (generally inhibiting SOA formation).[10] Isomerization forms a peroxy radical, which will react with NO to form either an alkyl nitrate (blue arrow) or another alkoxy radical. This newly formed alkoxy radical will mostly "back-isomerize" to form a hydroxycarbonyl, though some fraction (∼10%) will instead "forward-isomerize", ultimately leading to the formation of a dihydroxycarbonyl or dihydroxynitrate.[19,24]

dx.doi.org/10.1021/jp506562r | J. Phys. Chem. A 2014, 118, 8807−8816

Table 1. Summary of SOA Yield Parameters and Elemental Ratio Measurements[a]

RO isomer	substitution	O/C	H/C	N/C	α_1 (c^* = 1 μg/m^3)	α_2 (c^* = 10 μg/m^3)	α_3 (c^* = 100 μg/m^3)
decyl-1-oxy	primary	**0.19**	**1.62**	**0.05**	**0.33**	**2.15**	**7.95**
decyl-2-oxy	secondary	0.23	1.60	0.05	0.23	0.47	9.55
decyl-4-oxy	secondary	0.32	1.61	0.03	0.27	0.58	6.25
decyl-3-oxy	secondary	0.32	1.61	0.03	0.22	0.00	7.89
decyl-5-oxy secondary	secondary	0.23	1.70	0.04	0.20	0.90	3.07
secondary average		**0.28 ± 0.05**	**1.63 ± 0.07**	**0.04 ± 0.01**	**0.23 ± 0.03**	**0.49 ± 0.37**	**6.69 ± 2.77**
2-methyl-2-nonyloxy	α-substituted	0.23	1.64	0.04	0.09	0.13	6.67
2-methyl-4-nonyloxy	γ-substituted	0.28	1.61	0.03	0.11	0.00	5.99
2-methyl-5-nonyloxy	δ-substituted	0.25	1.66	0.03	0.11	0.00	5.99
5-methyl-5-nonyloxy	α-substituted	0.21	1.66	0.03	0.14	0.00	4.76
4-methyl-5-nonyloxy	β-substituted	0.25	1.64	0.03	0.06	0.39	2.68
3,4-diethyl-3-hexyloxy[b]	α,β-disubstituted	–	–	–	–	–	–
branched average[c]		**0.24 ± 0.03**	**1.64 ± 0.02**	**0.03 ± 5 × 10^{-3}**	**0.10 ± 0.03**	**0.10 ± 0.17**	**5.22 ± 1.58**

[a]Species are listed in order of decreasing yields. Mass-based yields (α) were derived using a three-product fitting with the volatility basis set for c^* (μg/m^3) = {1, 10, 100}. Averages are reported as ±1σ. [b]SOA formation not observed. [c]Average of values for all branched alkoxy radicals except 3,4-diethyl-3-hexyloxy.

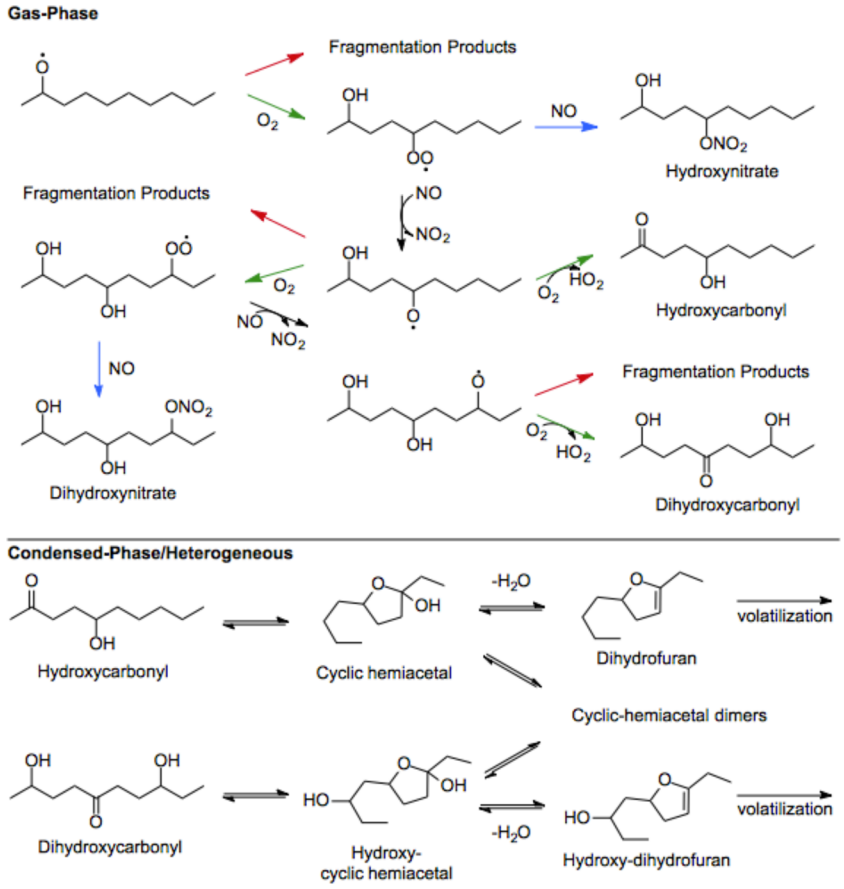

Figure 5. Formation of first-generation products from a single alkoxy radical species. Shown are the major gas-phase (top panel) and condensed phase/heterogeneous (bottom panel) reactions and products formed from a representative alkoxy radical, decyl-2-oxy. Alkoxy radicals will fragment (red arrow) or isomerize (green arrow); isomerization leads to the formation of a peroxy radical, which in the presence of NO can form an organonitrate (blue arrow) or a new alkoxy radical, opening up additional isomerization and fragmentation channels.

The lower panel of Figure 5 shows the subsequent heterogeneous and condensed-phase reactions available to (di)hydroxycarbonyls, which can undergo heterogeneous cyclization to form (hydroxy)cyclic hemiacetals.[10,11,19] Such compounds can dimerize to form hemiacetal dimers or dehydrate to form a (hydroxy)dihydrofuran. This latter compound is volatile and will likely partition into the gas phase, where (if oxidants are present) it will rapidly react to form second-generation oxidation products.[25]

High molecular weight (m/z > 150 Da) ion fragments were observed in all mass spectra, and the chemical formulas of major ions were determined by high-resolution analysis (Figure 6). All

dx.doi.org/10.1021/jp506562r | J. Phys. Chem. A 2014, 118, 8807−8816

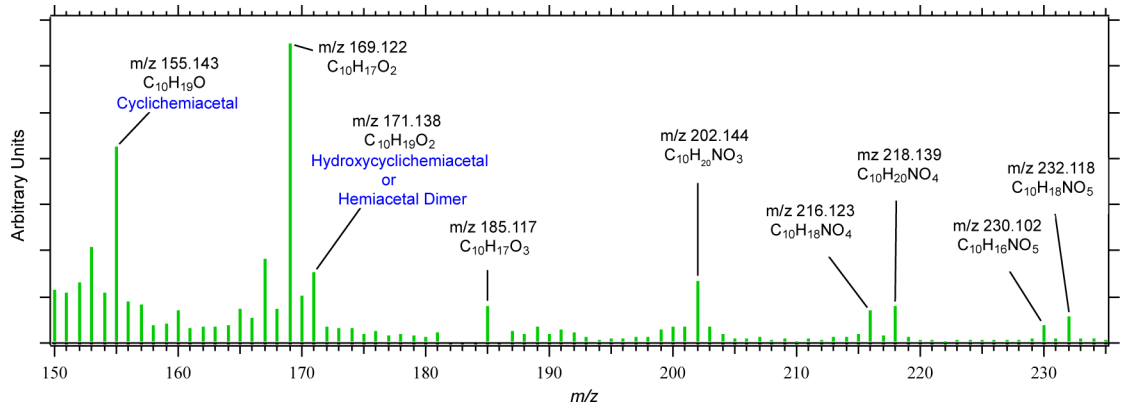

Figure 6. High-mass ions (m/z 150–235) in the AMS spectrum of SOA formed from decyl-1-nitrite photolysis. Ion formulas given were confirmed by high-resolution analysis; tentative molecular assignments are from Lim and Ziemann.[19]

such ions have 10 carbon atoms, and most are the C_{10} analogs of ions previously observed in alkane + OH experiments by Lim and Ziemann;[19] the exact masses measured using high-resolution mass spectrometry confirm the identification of the ion formulas suggested in that study. Three of the most abundant fragments correspond to species with 10 carbon atoms and 1–2 oxygen atoms, m/z 155.143 ($C_{10}H_{19}O^+$), 169.122 ($C_{10}H_{17}O_2^+$), and 171.138 ($C_{10}H_{19}O_2^+$). The time series of each fragment from representative primary, secondary, and branched nitrite photolysis experiments are shown in Figure 7. Fragment

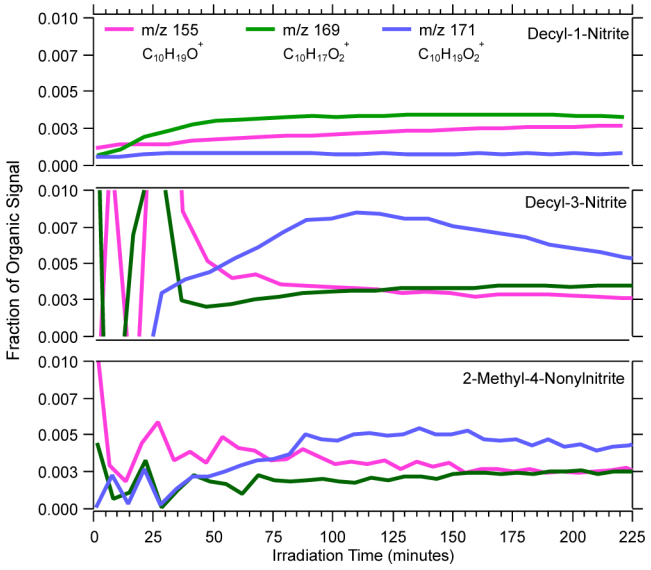

Figure 7. Ion time series for three of the major ions, m/z 155.143, 169.122, and 171.138, for a representative primary (decyl-1-nitrite), secondary (decyl-3-nitrite), and branched (2-methyl-4-nonylnitrite) experiment. Traces are shown as a fraction of the total organic mass.

abundances (shown as the fraction of the organic signal) increase immediately following irradiation and level off after 1.5–3 h, with the exception of $C_{10}H_{19}O_2^+$, which peaks and then decreases slightly.

Although definitive assignments of the parent molecular product species are not possible using the AMS, tentative assignments can be made on the basis of the work of Lim and Ziemann.[19] The $C_{10}H_{19}O^+$ and $C_{10}H_{19}O_2^+$ ions may correspond to two major first-generation products, the cyclic hemiacetal (m/z 155.143) and the hydroxy-cyclic hemiacetal or hemiacetal dimer (m/z 171.138), respectively. The $C_{10}H_{17}O_2^+$ ion (m/z 169.122) has previously been identified as the cyclichemiacetal nitrate, a second-generation oxidation product.[11] This may indicate the importance of multigenerational oxidation processes, as discussed below, though this fragment ion may not be unique to this one product. Furthermore, several prominent N-containing ions of m/z > 200 are present, pointing to the presence of organonitrate species; the detailed molecular assignments for such species are unclear at present. The absence of abundant ions corresponding to the hydroxycarbonyl, hydroxynitrate, and dihydrofuran (which would be found at m/z 154, 138, and 140 respectively)[19] is likely due to the high volatilities of such species. Unfortunately, low ion intensities and unknown ionization efficiencies preclude the detailed interpretation of the high-mass ions in the AMS spectra, and in particular their relative product yields in different alkoxy radical experiments. Nonetheless, the observation of ions similar to those observed by Lim and Ziemann[19] provides strong confirmation that the present experiments access the chemistry important in the early generation oxidation of alkanes.

Role of Multigenerational Oxidation. The mechanism shown in Figure 5 includes no oxidation of the reaction products; in standard (oxidant-initiated) studies of SOA, reaction products will react further with oxidants, leading to a complex mixture of multigenerational products. By contrast, in the present chemical system (the photolytic generation of radicals), all chemistry is initiated without oxidants, allowing for individual oxidation steps to be studied in greater detail than in oxidant-initiated studies. Nonetheless, some additional oxidation may occur in the present studies via the secondary generation of oxidants. Oxidation by NO_3 and O_3 is unlikely, due to the high (ppm) levels of NO present. However, because HO_2 can be formed via isomerization reactions (Figure 5), some OH formation may occur via the HO_2 + NO reaction. Though some of the OH formed will react with NO_2 to form HNO_3, most will likely react with the organic products formed (and early in the reaction, possibly even the nitrite as well). The importance of OH-initiated secondary chemistry can be examined from the behavior of the $C_{10}H_{19}O^+$ (m/z 155.143) ion, previously assigned to the cyclic hemiacetal species.[11,25] Because this compound is in equilibrium with the highly reactive dihydrofuran (Figure 5), the presence of oxidants will lead to a rapid depletion of that ion. However, as shown in Figure 7, no such depletion is observed, in stark contrast to results from alkane oxidation studies.[11,25] Although this might indicate that OH-initiated chemistry is unimportant in the present system, it is also possible that the stable concentration of

dx.doi.org/10.1021/jp506562r | J. Phys. Chem. A 2014, 118, 8807–8816

the species arises from the absence of sufficient HNO_3 to catalyze the dehydration of the cyclichemiacetal. Furthermore, the assignment of the $C_{10}H_{19}O^+$ ion to the cyclichemiacetal is tentative, and this ion instead may correspond to some other product. By contrast, the $C_{10}H_{19}O_2^+$ ion (m/z 171.138) does indeed decrease to some extent; this could indicate oxidation of the hydroxy-cyclic hemiacetal, though it may instead be a result of nonoxidative chemistry of the hemiacetal dimer.

Differences in SOA yields and properties measured in the present study and those in the analogous *n*-decane + OH reaction[18,20,21,26] provide additional insight into the role of multigenerational oxidation in our experiments. In particular, SOA yields from OH + *n*-decane are substantially higher than those from the RONO photolysis. Shown in Figure 4 is the SOA yield measured by Presto et al.[18] (green diamond). This yield falls between those measured in this study from decyl-1-oxy and decyl-2-oxy radicals, and thus is substantially higher than the yields inferred from the RONO experiments (because these two radicals together account for only ~24% of the first alkoxy radical isomers formed in the *n*-decane + OH reaction[27]). The difference in aerosol formation between these two studies is even more pronounced than is implied from these yield differences, given that decyl nitrate, a volatile first-generation product from OH + *n*-decane, is not formed from RONO photolysis. Studies of OH + *n*-decane carried out at higher OH exposures than accessed by Presto et al.[18] found even higher SOA yields (>10%),[20,21] consistent with additional OH oxidation leading to more SOA formation (the experiments from Lim and Ziemann[19] were carried out at much higher c_{OA}, preventing a direct comparison with our results here). Similar differences are seen in the degree of oxidation of SOA; O/C ratios measured in this work are lower (0.19−0.32) on average than those from OH + *n*-decane (0.33−0.35),[21,26] whereas H/C ratios are higher (1.6−1.7 versus 1.5−1.6).[21,26] These results all suggest that, relative to OH-initiated SOA studies, multigenerational oxidation chemistry is suppressed in the present experiments, with the formation of SOA that is more heavily weighted toward first-generation oxidation products.

Effect of Alkoxy Radical Structure on SOA Formation. The large variability in yields and chemical composition of SOA formed from various C_{10} alkoxy radical isomers (Figure 3 and Table 1) underscores the high degree of sensitivity of SOA formation to the exact chemical structure of the precursor species. The location and degree of substitution of the alkoxy radical center appears to have a governing effect on observed yields this is particularly evident in the large differences in yields among the various radicals with straight-chain carbon skeletons and between the structurally similar 2-methyl-2-nonyloxy and 5-methyl-5-nonyloxy radicals. As described below, differences in the yield and composition of SOA from the different isomeric alkoxy radicals can be explained in terms of two general factors, the branching between fragmentation and isomerization of the alkoxy radicals (including those formed subsequent to isomerization) and the relative volatilities of the different isomeric products formed from each radical.

Alkoxy Radical Products. The exact chemical structure of each alkoxy radical has a governing influence on the reactive pathways available to it, which in turn can affect the amount and composition of SOA formed.[5,10,11] Using a structure−activity relationship (SAR) to describe alkoxy radical reactivity,[24] and in particular the branching between isomerization (functionalization) and C−C bond scission (fragmentation), we calculated the distribution of first-generation products from each alkoxy radical studied. Such calculations take into account the fate of not only the original alkoxy radical but also any alkoxy radical formed later in the reaction sequence (Figure 5); calculation details are given in the Supporting Information.

The calculated product distributions for the major first-generation products of each alkoxy radical isomer are shown in Figure 8. For most of the alkoxy radicals studied, hydroxynitrates

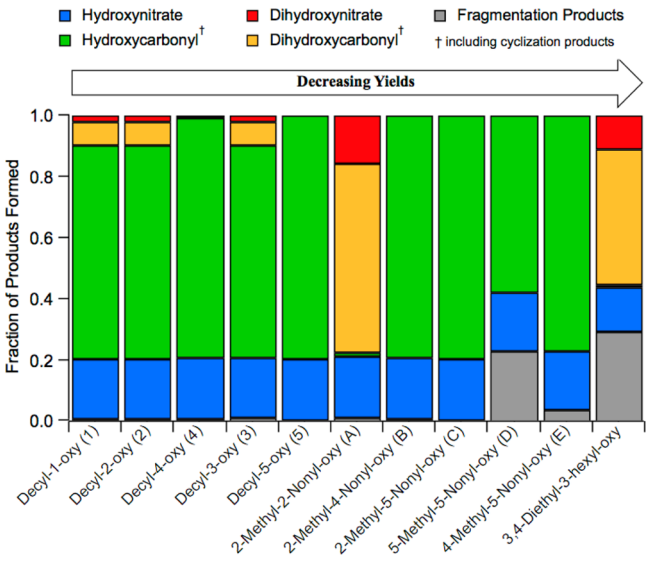

Figure 8. Distribution of major first-generation products from each alkoxy radical isomer. Isomers are listed in order of decreasing yields, and the identifiers in parentheses correspond to those used in Figure 4. Product distributions are estimated using structure−activity relationships, as described in the Supporting Information.

and hydroxycarbonyls are the major products. The predicted product distributions from decyl-1-oxy, decyl-2-oxy, and decyl-3-oxy are identical. For these species, the formation of fragmentation products is negligible (<3%), whereas products arising from multiple isomerization reactions (dihydroxycarbonyls and dihydroxynitrates) represent a small but significant (~10%) fraction of the total products. The predicted products from the other two straight-chain radicals (decyl-4-oxy and decyl-5-oxy) are similar, though they do not include the dihydroxy species, because "forward-isomerization" reactions either cannot occur (due to the lack of H atoms in the δ-position) or are highly unfavorable (due to the δ-H atoms residing on methyl groups). The lack of formation of these low-volatility products may contribute somewhat to their lower SOA yields. However, because the SOA yield from the decyl-4-oxy radical is somewhat greater than that from the decyl-3-oxy radical, this appears to be a minor effect.

Estimated product distributions from the δ- and γ-substituted branched species (2-methyl-5-nonyloxy and 2-methyl-4-nonyloxy, respectively) are similar to those of the straight-chain species, because the branch points are located relatively far from the alkoxy radical center and thus have little influence on the chemistry. The other branched alkoxy radicals, however, are predicted to form very different sets of products; these can include fragmentation products, which can at least partly explain their lower SOA yields. The two α-substituted branched species (2-methyl-2-nonyloxy and 5-methyl-5-nonyloxy), despite being quite similar structurally, have dramatically different product distributions, due to the number of isomerization reactions available to each. 2-Methyl-2-nonyloxy is unable to form a

dx.doi.org/10.1021/jp506562r | J. Phys. Chem. A 2014, 118, 8807−8816

hydroxycarbonyl, because the α-substituted methyl group prevents "back-isomerization"; however, it is able to undergo a second "forward-isomerization" that 5-methyl-5-nonyloxy cannot. Instead, the second alkoxy radical formed from 5-methyl-5-nonlyoxy will react with O_2 to form a significant amount of hydroxycarbonyl species (~50%). The result is that the products of the 2-methyl-2-nonyloxy radical are dominated by the low-volatility dihydroxy species (~80%), whereas those from 5-methyl-5-nonyloxy are fragmentation products (25%), alkyl nitrates (~25%), or hydroxycarbonyls (~50%) formed from the RO + O_2 pathway. This is consistent with 2-methyl-2-nonyloxy having the highest yields among the branched isomers, and 5-methyl-5-nonyloxy among the lowest.

The lowest SOA yields measured were from the β-substituted species, 4-methyl-5-nonyloxy (mono-β-substituted) and 3,4-diethyl-3-hexyloxy (α,β-disubstituted, for which no SOA formation was observed), suggesting a high degree of radical fragmentation in those cases. However, the amount of fragmentation predicted by the SAR is relatively modest (4% from 4-methyl-5-nonyloxy and 30% from 3,4-diethyl-3-hexyloxy). This difference suggests that fragmentation of β-substituted alkoxy radicals may be underestimated using the SAR, which estimates fragmentation based upon reaction enthalpy;[24] this may result from the lack of accurate values of reaction enthalpies of secondary β-substituted alkoxy radicals. An alternate SAR for describing alkoxy radical fragmentation, based on the degree of substitution of the α- and β-carbon atoms,[28] predicts substantially more fragmentation (57% and 94% from 4-methyl-5-nonyloxy and 3,4-diethyl-3-hexyloxy, respectively). This is in better agreement with the SOA trends observed, though fragmentation of 4-methyl-5-nonyloxy may still be underestimated. Moreover, this SAR also predicts increased fragmentation of α-substituted radicals, which is not consistent with the relatively high SOA yields from those species (Supporting Information). Both SARs are based upon measurements of fragmentation rates of relatively small alkoxy radicals; this work suggests the need for the direct study of the fate of larger, more substituted radicals to better constrain such descriptions of alkoxy radical chemistry.

Volatility of SOA Components. As described above, the extent of alkoxy radical fragmentation and isomerization are in good qualitative agreement with many of the observed differences in yields, particularly for the branched species. However, the differences in yields among the straight-chain species (which are predicted to have very similar product distributions) and the relatively low O/C values for decyl-1-oxy and decyl-2-oxy, are not captured by this explanation alone, pointing to additional factors controlling SOA formation. These appear to be related to differences in the volatilities of the (isomeric) products formed. As shown in Table 1, SOA from the secondary and branched radicals exhibit volatility distributions that are skewed toward higher c^* relative to the SOA from primary radicals, as reflected in differences in both α_1/α_{100} and α_{10}/α_{100} ratios. This effect can also be seen in Figure 4, which shows that the relative differences among yields from different radical types are most pronounced at low values of c_{OA}.

Such differences in SOA volatility, even when formation occurs via similar chemistry (i.e., from straight-chain isomers), likely arise from differences in vapor pressures of the isomeric product species. Although the various precursor alkoxy radicals and their products (hydroxycarbonyls, hydroxynitrates, etc.) have the same chemical formulas, their spatial arrangement can lead to large differences in their relative volatilities. Among the straight-chain radicals, yields tend to increase as the alkoxy radical center is located closer to the terminus of the molecule. (The one exception is decyl-3-oxy, which has lower yields than decyl-4-oxy; however, such a difference is small.) This effect likely arises from the fact that functional groups located closer to the terminus of molecules generally have larger influences on vapor pressure, because the molecules can "stack" more efficiently. For example, for straight-chain C_9 alcohols, the vapor pressure of 1-nonanol is 5 times lower than that of 2-nonanol, which in turn is 1.4 times lower than the vapor pressures of the remaining isomers (the differences among 3-nonanol, 4-nonanol, and 5-nonanol are much smaller, under 5%).[29] The relative ordering of SOA yields among the straight-chain alkoxy radicals is broadly consistent with this trend, pointing to the role of the volatilities of product isomers on SOA formation. In addition, the formation of aldehydes (terminal carbonyls), which have slightly lower volatilities than ketones formed by secondary alkoxy radicals,[1] and which are also more susceptible to oligomerization reactions (such as hemiacetal formation),[30] further decreases volatility. Because the primary decyl-1-oxy species is the only isomer capable of forming aldehydes, its products are lower in volatility, explaining its higher values of α_1/α_{100} relative to those from the secondary and branched isomers. Similarly, the structure of the carbon skeleton may play a role, because branched species generally have higher volatilities than straight-chain isomers. This "P_{25} effect"[10] may contribute to the low yields from branched alkoxy radicals; however, differences in alkoxy radical fragmentation (as described above) are likely the dominant factor for most of the isomers studied.

Such differences in volatilities of different product isomers may also explain some of the trends in O/C ratios, particularly among the straight-chain radicals, because products from the decyl-1-oxy and decyl-2-oxy are lower in volatility relative to corresponding isomers from the other alkoxy radicals. This enhances the gas-to-particle partitioning of less oxidized (less functionalized) products, resulting in lower O/C of the aerosol.[31] It may also explain the increased abundance of organonitrate species, evident by higher N/C, in SOA that is the least oxidized (lowest O/C).

CONCLUSIONS

In the present work we highlight several important structural features of alkoxy radical structure that influence the SOA-forming potential of straight-chain and branched alkanes. The use of photolytically generated alkoxy radicals allows for the isolation of individual reaction pathways and oxidation generations, permitting the examination of the role of chemical structure in more detail than is typically possible in oxidant-initiated SOA studies. Measurements of SOA yields and composition broadly agree with previous work on the OH initiated oxidation of alkanes, indicating the relevance of this work to that important chemical system. However, both SOA yields and chemical composition are found to vary dramatically with alkoxy radical structure, even for those sharing the same carbon skeleton (e.g., the five unbranched isomers, decyl-1-oxy through decyl-5-oxy). Such differences can largely be explained in terms of (1) the complex branching between reaction pathways available to the alkoxy radical and (2) the role of functional group position and carbon skeleton on the volatility of the oxidation products. These SOA measurements also provide some insight into the role of structure on alkoxy radical reactivity; in particular, the very low SOA yields from the β-substituted

dx.doi.org/10.1021/jp506562r | J. Phys. Chem. A 2014, 118, 8807−8816

alkoxy radicals suggest more fragmentation than is predicted by commonly used structure−activity relationships.[28,32]

More generally, the study of aerosol formation from single radical species enables the importance of individual reaction pathways and products in SOA formation to be examined in detail. For systems whose yields of condensable species are low (such as the first-generation oxidation of C_{10} hydrocarbons, studied here), products that are formed in small yields may still play a major role in SOA formation. For example, for the straight-chain structures studied, the primary radical (decyl-1-oxy) was found to form more SOA than any of the secondary ones. In the analogous OH + *n*-decane reaction, the formation of this radical (via abstraction at the terminal carbon) accounts for only ∼4% of the total reaction;[27] however, the fractional contribution of this channel to the total SOA formed is likely to be substantially higher than this. Ultimately, the identification of these key channels and their products is necessary for relating the amounts and properties of SOA to the structure of a given precursor compound.

■ ASSOCIATED CONTENT

Supporting Information

Details of the branching ratio calculation (as shown in Figure 8), including a figure of radical branching, tables of isomerization and fragmentation rate constants, and a graph of first-generation product distributions calculated by an alternative SAR, are given in the Supporting Information. The material is available free of charge via the Internet at http://pubs.acs.org.

■ AUTHOR INFORMATION

Corresponding Author

*Jesse H. Kroll. E-mail: jhkroll@mit.edu.

Notes

The authors declare no competing financial interest.

■ ACKNOWLEDGMENTS

This work was supported by the National Science Foundation under grant number CHE-1012809. We thank Roger Summons for use of the GC for confirmation of nitrite identities following synthesis and Paul Ziemann for helpful discussions.

■ REFERENCES

(1) Kroll, J. H.; Seinfeld, J. H. Chemistry of Secondary Organic Aerosol: Formation and Evolution of Low-Volatility Organics in the Atmosphere. *Atmos. Environ.* **2008**, *42*, 3593−3624.

(2) Hallquist, M.; Wenger, J. C.; Baltensperger, U.; Rudich, Y.; Simpson, D.; Claeys, M.; Dommen, J.; Donahue, N. M.; George, C.; Goldstein, A. H.; et al. The Formation, Properties and Impact of Secondary Organic Aerosol: Current and Emerging Issues. *Atmos. Chem. Phys.* **2009**, *9*, 5155−5236.

(3) Kroll, J. H.; Donahue, N. M.; Jimenez, J. L.; Kessler, S. H.; Canagaratna, M. R.; Wilson, K. R.; Altieri, K. E.; Mazzoleni, L. R.; Wozniak, A. S.; Bluhm, H.; et al. Carbon Oxidation State as a Metric for Describing the Chemistry of Atmospheric Organic Aerosol. *Nat. Chem.* **2011**, *3*, 133−139.

(4) Goldstein, A. H.; Galbally, I. E. Known and Unexplored Organic Constituents in the Earth's Atmosphere. *Environ. Sci. Technol.* **2007**, *41*, 1514−1521.

(5) Ziemann, P. J.; Atkinson, R. Kinetics, Products, and Mechanisms of Secondary Organic Aerosol Formation. *Chem. Soc. Rev.* **2012**, *41*, 6582−6605.

(6) Kessler, S. H.; Nah, T.; Carrasquillo, A. J.; Jayne, J. T.; Worsnop, D. R.; Wilson, K. R.; Kroll, J. H. Formation of Secondary Organic Aerosol from the Direct Photolytic Generation of Organic Radicals. *J. Phys. Chem. Lett.* **2011**, *2*, 1295−1300.

(7) Morabito, P.; Heicklen, J. Primary Photochemical Processes in the Photolysis of Alkyl Nitrites at 366nm and 23C in the Presence of ^{15}NO. *Int. J. Chem. Kinet.* **1985**, *17*, 535−546.

(8) Heicklen, J. The Decomposition of Alkyl Nitrites and the Reaction of Alkoxy Radicals. *Adv. Photochem.* **1988**, *14*, 177−272.

(9) Orlando, J. J.; Tyndall, G. S.; Bilde, M.; Ferronato, C.; Wallington, T. J.; Vereecken, L.; Peeters, J. Laboratory and Theoretical Study of the Oxy Radicals in the OH- and Cl-Initiated Oxidation of Ethene. *J. Phys. Chem. A* **1998**, *102*, 8116−8123.

(10) Lim, Y. B.; Ziemann, P. J. Effects of Molecular Structure on Aerosol Yields from OH Radical-Initiated Reactions of Linear, Branched, and Cyclic Alkanes in the Presence of NO_x. *Environ. Sci. Technol.* **2009**, *43*, 2328−2334.

(11) Lim, Y. Bin; Ziemann, P. J. Products and Mechanism of Secondary Organic Aerosol Formation from Reactions of n-Alkanes with OH Radicals in the Presence of NO_x. *Environ. Sci. Technol.* **2005**, *39*, 9229−9236.

(12) Noyes, W. A. Explanation of the Formation of Alkyl Nitrites in Dilute Solutions; Butyl and Amyl Nitrites. *J. Am. Chem. Soc.* **1933**, *55*, 3888−3889.

(13) DeCarlo, P. F.; Kimmel, J. R.; Trimborn, A.; Northway, M. J.; Jayne, J. T.; Aiken, A. C.; Gonin, M.; Fuhrer, K.; Horvath, T.; Docherty, K. S.; et al. Field-Deployable, High-Resolution, Time-of-Flight Aerosol Mass Spectrometer. *Anal. Chem.* **2006**, *78*, 8281−8289.

(14) Aiken, A. C.; DeCarlo, P. F.; Jimenez, J. L. Elemental Analysis of Organic Species with Electron Ionization High-Resolution Mass Spectrometry. *Anal. Chem.* **2007**, *79*, 8350−8358.

(15) Aiken, A. C.; Decarlo, P. F.; Kroll, J. H.; Worsnop, D. R.; Huffman, J. A.; Docherty, K. S.; Ulbrich, I. M.; Mohr, C.; Kimmel, J. R.; Sueper, D.; et al. O/C and OM/OC Ratios of Primary, Secondary, and Ambient Organic Aerosols with High-Resolution Time-of-Flight Aerosol Mass Spectrometry. *Environ. Sci. Technol.* **2008**, *42*, 4478−4485.

(16) Hildebrandt, L.; Donahue, N. M.; Pandis, S. N. High Formation of Secondary Organic Aerosol from the Photo-Oxidation of Toluene. *Atmos. Chem. Phys.* **2009**, *9*, 2973−2986.

(17) Zhang, X.; Cappa, C. D.; Jathar, S. H.; McVay, R. C.; Ensberg, J. J.; Kleeman, M. J.; Seinfeld, J. H. Influence of Vapor Wall Loss in Laboratory Chambers on Yields of Secondary Organic Aerosol. *Proc. Natl. Acad. Sci. U. S. A.* **2014**, *111*, 5802−5807.

(18) Presto, A. A.; Miracolo, M. A.; Donahue, N. M.; Robinson, A. L. Secondary Organic Aerosol Formation from High-NO_x Photo-Oxidation of Low Volatility Precursors: n-Alkanes. *Environ. Sci. Technol.* **2010**, *44*, 2029−2034.

(19) Lim, Y. B.; Ziemann, P. J. Chemistry of Secondary Organic Aerosol Formation from OH Radical-Initiated Reactions of Linear, Branched, and Cyclic Alkanes in the Presence of NO_x. *Aerosol Sci. Technol.* **2009**, *43*, 604−619.

(20) Lambe, A. T.; Onasch, T. B.; Croasdale, D. R.; Wright, J. P.; Martin, A. T.; Franklin, J. P.; Massoli, P.; Kroll, J. H.; Canagaratna, M. R.; Brune, W. H.; et al. Transitions from Functionalization to Fragmentation Reactions of Laboratory Secondary Organic Aerosol (SOA) Generated from the OH Oxidation of Alkane Precursors. *Environ. Sci. Technol.* **2012**, *46*, 5430−5437.

(21) Hunter, J. F.; Carrasquillo, A. J.; Daumit, K. E.; Kroll, J. H. Secondary Organic Aerosol Formation from Acyclic, Monocyclic, and Polycyclic Alkanes. *Environ. Sci. Technol.* **2014**, *48*, 10227−10234.

(22) Donahue, N. M.; Robinson, A. L.; Stanier, C. O.; Pandis, S. N. Coupled Partitioning, Dilution, and Chemical Aging of Semivolatile Organics. *Environ. Sci. Technol.* **2006**, *40*, 2635−2643.

(23) Farmer, D. K.; Matsunaga, A.; Docherty, K. S.; Surratt, J. D.; Seinfeld, J. H.; Ziemann, P. J.; Jimenez, J. L. Response of an Aerosol Mass Spectrometer to Organonitrates and Organosulfates and Implications for Atmospheric Chemistry. *Proc. Natl. Acad. Sci. U. S. A.* **2010**, *107*, 6670−6675.

(24) Atkinson, R. Rate Constants for the Atmospheric Reactions of Alkoxy Radicals: An Updated Estimation Method. *Atmos. Environ.* **2007**, *41*, 8468−8485.

(25) Lim, Y. Bin; Ziemann, P. J. Kinetics of the Heterogeneous Conversion of 1,4-Hydroxycarbonyls to Cyclic Hemiacetals and Dihydrofurans on Organic Aerosol Particles. *Phys. Chem. Chem. Phys.* **2009**, *11*, 8029−8039.
(26) Tkacik, D. S.; Presto, A. A.; Donahue, N. M.; Robinson, A. L. Secondary Organic Aerosol Formation from Intermediate-Volatility Organic Compounds: Cyclic, Linear, and Branched Alkanes. *Environ. Sci. Technol.* **2012**, *46*, 8773−8781.
(27) Atkinson, R. A Structure-Activity Relationship for the Estimation of Rate Constants for the Gas-Phase Reactions of OH Radicals with Organic Compounds. *Int. J. Chem. Kinet.* **1987**, *19*, 799−828.
(28) Peeters, J.; Fantechi, G.; Vereecken, L. A Generalized Structure-Activity Relationship for the Decomposition of (Substituted) Alkoxy Radicals. *J. Atmos. Chem.* **2004**, *48*, 59−80.
(29) Verevkin, S. P.; Schick, C. Vapour Pressures and Heat Capacity Measurements on the C7−C9 Secondary Aliphatic Alcohols. *J. Chem. Thermodyn.* **2007**, *39*, 758−766.
(30) Jang, M.; Czoschke, N. M.; Lee, S.; Kamens, R. M. Heterogeneous Atmospheric Aerosol Production by Acid-Catalyzed Particle-Phase Reactions. *Science* **2002**, *298*, 814−817.
(31) Shilling, J. E.; Chen, Q.; King, S. M.; Rosenoern, T.; Kroll, J. H.; Worsnop, D. R.; DeCarlo, P. F.; Aiken, A. C.; Sueper, D.; Jimenez, J. L.; et al. Loading-Dependent Elemental Composition of α-Pinene SOA Particles. *Atmos. Chem. Phys.* **2009**, *9*, 771−782.
(32) Atkinson, R. Rate Constants for the Atmospheric Reactions of Alkoxy Radicals: An Updated Estimation Method. *Atmos. Environ.* **2007**, *41*, 8468−8485.